Video Article

Three-dimensional Optical-resolution Photoacoustic Microscopy

Song Hu, Konstantin Maslov, Lihong V. Wang
Optical Imaging Laboratory, Department of Biomedical Engineering, Washington University in St. Louis

Correspondence to: Lihong V. Wang at lhwang@biomed.wustl.edu

URL: http://www.jove.com/details.php?id=2729
DOI: 10.3791/2729
Citation: Hu S., Maslov K., Wang L.V. (2011). Three-dimensional Optical-resolution Photoacoustic Microscopy. JoVE. 51. http://www.jove.com/details.php?id=2729, doi: 10.3791/2729

Abstract

Optical microscopy, providing valuable insights at the cellular and organelle levels, has been widely recognized as an enabling biomedical technology. As the mainstays of *in vivo* three-dimensional (3-D) optical microscopy, single-/multi-photon fluorescence microscopy and optical coherence tomography (OCT) have demonstrated their extraordinary sensitivities to fluorescence and optical scattering contrasts, respectively. However, the optical absorption contrast of biological tissues, which encodes essential physiological/pathological information, has not yet been assessable.

The emergence of biomedical photoacoustics has led to a new branch of optical microscopy optical-resolution photoacoustic microscopy (OR-PAM)[1], where the optical irradiation is focused to the diffraction limit to achieve cellular[1] or even subcellular[2] level lateral resolution. As a valuable complement to existing optical microscopy technologies, OR-PAM brings in at least two novelties. First and most importantly, OR-PAM detects optical absorption contrasts with extraordinary sensitivity (i.e., 100%). Combining OR-PAM with fluorescence microscopy[3] or with optical-scattering-based OCT[4] (or with both) provides comprehensive optical properties of biological tissues. Second, OR-PAM encodes optical absorption into acoustic waves, in contrast to the pure optical processes in fluorescence microscopy and OCT, and provides background-free detection. The acoustic detection in OR-PAM mitigates the impacts of optical scattering on signal degradation and naturally eliminates possible interferences (i.e., crosstalks) between excitation and detection, which is a common problem in fluorescence microscopy due to the overlap between the excitation and fluorescence spectra.

Unique for optical absorption imaging, OR-PAM has demonstrated broad biomedical applications since its invention, including, but not limited to, neurology[5, 6], ophthalmology[7, 8], vascular biology[9], and dermatology[10]. In this video, we teach the system configuration and alignment of OR-PAM as well as the experimental procedures for *in vivo* functional microvascular imaging.

Protocol

1. System configuration

1. Optical irradiation
    1. Optical irradiation source: a diode-pumped solid-state pulsed laser (INNOSLAB, Edgewave) and a dye laser (CBR-D, Sirah).
    2. The output laser beam (pulse width: 7 ns) is focused by a condenser lens (LA1131, Thorlabs) to pass through a 50-μm pinhole (P50C, Thorlabs).
    3. The pinhole is positioned slightly away from the focus of the condenser lens to match the pinhole diameter with the fundamental-mode beam diameter for effective spatial filtering.
    4. The filtered beam is attenuated by a neutral-density filter (NDC-50C-2M, Thorlabs) and then coupled into a single-mode optical fiber (P1-460A-FC-2, Thorlabs).
    5. The fiber output fills the back aperture of a microscope objective (RMS4X, Thorlabs) to achieve a diffraction-limited optical focus of ~2.6 μm at the wavelength of 570 nm.

2. Ultrasonic detection
    1. Ultrasonic transducer: 50-MHz central frequency (V214-BB-RM, Olympus-NDT).
    2. The ultrasonic transducer is attached to a home-made acoustic-optical beam combiner[11] for ultrasonic detection, which is aligned coaxially with the diffraction-limited optical irradiation.
    3. A spherical cavity is ground out of the bottom of the combiner to produce an acoustic lens. This acoustic lens has a numerical aperture of 0.5 in water and gives an acoustic focal diameter of 43 μm at the 50-MHz central frequency.
    4. The optical and acoustic foci are aligned confocally to maximize the detection sensitivity.

3. Acoustic coupling
    1. Dry ultrasonic coupling is employed to avoid submerging experimental animals in water, which was used in early photoacoustic imaging systems[12].
    2. An imaging window is opened in the bottom of a Petri dish (9 cm in diameter) and is sealed with an ultrasonically and optically transparent polyethylene membrane.
    3. Ultrasonic gel (Clear Image, SonoTech) between the polyethylene membrane and the object to be imaged couples the generated photoacoustic wave from the object to the Petri dish, and deionized water in the Petri dish further couples the wave to the submerged OR-PAM imaging head.

4. Electronics
    1. The photoacoustic signal detected by the ultrasonic transducer is amplified by two cascaded amplifiers (ZFL 500LN, Mini-Circuits)
    2. The amplified signal is digitized by a 14-bit data acquisition (DAQ) board (CompuScope 14200, Gage Applied Sciences) at a sampling rate of 200 MS/s.

5. Scanning scheme
    1. Two-dimensional (2-D) raster scanning of the OR-PAM imaging head along the horizontal (x-y) plane is controlled by a personal computer, which triggers both the DAQ board and the pump laser. The trigger signal is synchronized with the clock-out signal from the DAQ board.
    2. The fast axis of the 2-D scanner is defined as the direction of the cross-sectional scan (B-scan).
    3. A sequence of B-scan images can be acquired by translating the imaging head along the slow axis to form a volumetric image, which can be viewed either in a direct 3-D rendering or in a 2-D maximum amplitude projection (MAP) image.

2. System alignment

1. Use pulse-echo ultrasound and an ultrasonic reflector to determine the position of the acoustic focal plane (i.e., the time delay from the trigger signal to the maximum pulse-echo ultrasonic signal). This step is required to be performed only once when building the OR-PAM system.
2. Maximize the coupling efficiency of the single-mode fiber.
3. Apply ultrasonic gel on top of an optically absorbing object (e.g., a piece of black tape) and gently attach it beneath the imaging window in the Petri dish filled with deionized water.
4. Lower the imaging head into the water, and remove air bubbles trapped under the acoustic lens.
5. Adjust the imaging head until the photoacoustic signal of the absorbing object is from the acoustic focal plane, which can be judged from the acoustic delay.
6. Adjust the vertical position (i.e., z position) of the microscope objective to maximize the amplitude of the photoacoustic signal generated from the flat object. The maximized signal amplitude suggests that the optical focus is aligned with the acoustic focus in the vertical direction.
7. Adjust the horizontal positions (i.e., x and y positions) of the microscope objective until the photoacoustic signal generated from the target shows a symmetric pattern. The symmetry suggests that the optical focus is aligned with the acoustic focus in the horizontal direction.
8. Repeat steps 2.6 and 2.7 until the photoacoustic signal is optimized in both symmetry and amplitude.

3. A sample experimental procedure-*in vivo* OR-PAM of mouse ear vasculature

1. *This step is not required for nude mice*. Anesthetize the animal with an intraperitoneal injection of a cocktail [recipe: 1 ml ketamine (100 mg/ml), 0.1 ml xylazine (100 mg/ml), and 8.9 ml saline; dosage: 0.1 ml/10 g]. Shave the hair in the ear, and further depilate the residual hair with Surgi Cream (Category #: 82565, American International Industries) before cleaning it with deionized water. Note that such depilation might slightly irritate the skin vasculature and thus is best performed 24 hours before the planned experiment.
2. Turn on the photoacoustic laser system, and check the system alignment.
3. Anesthetize the mouse with 3% isoflurane vaporized by the inhalation gas (the typical flow rate is 1.0-1.5 l/min, depending on the animal's body weight), and maintain the anesthesia with 1% isoflurane throughout the experiment. Medical-grade air is recommended as the inhalation gas to maintain the mouse at normal physiological status.
4. Transfer the mouse to a stereotactic stage, and control its body temperature at 37 °C with a heating pad.
5. Flatten the mouse ear on a plastic plate and apply a layer of ultrasound gel on top of the ear. Avoid trapping air bubbles inside the gel. Then, place the ear under the imaging window and slowly raise the animal stage until the ultrasound gel contacts the bottom of the polyethylene membrane. Soft contact is required because pressing the ear against the membrane may affect blood flow in the ear.
6. Clamp a pulse oximeter to the mouse leg or tail to monitor its physiological status, and apply ointment to the eyes to prevent dryness and accidental laser damage to the mouse eyes.
7. Lower the imaging head until the acoustic lens is immersed in deionized water, and remove air bubbles trapped under the acoustic lens.
8. Check the laser fluence to make sure it is within the laser safety standards of the American National Standards Institute[13]. The laser fluence should not exceed 20 mJ/cm^2, which translates into 80 nJ of laser pulse energy when the laser beam is focused at 150 μm beneath the skin surface.
9. Set the laser to the external-trigger mode and start trial scanning. Adjust the z position of the imaging head until the strongest photoacoustic signal is from the acoustic focal plane.
10. Set correct scanning parameters and start formal image acquisition.
11. After the experiment, turn off the laser, lift the imaging head out of the deionized water, lower the animal stage to release the mouse, clean the mouse ear with deionized water, turn off the anesthesia system and the temperature controller, and unload the mouse from the stereotactic stage.
12. If repetitive imaging is required, put the mouse in an incubator with the environmental temperature set at 37 °C. Return the mouse to the animal facility after it wakes up naturally. Otherwise, follow the animal protocols to euthanatize and dispose of it.

4. Functional OR-PAM of total concentration and oxygen saturation of hemoglobin

1. Oxyhemoglobin (HbO_2) and deoxyhemoglobin (HbR) are the two major forms of hemoglobin, the predominant endogenous photoacoustic source in the visible spectral range. HbO_2 and HbR have distinct optical absorption spectra and thus can be spectrally differentiated to quantify both the total concentration (HbT) and oxygen saturation (sO_2) of hemoglobin[5]. Here are two guidelines to help select proper optical wavelengths for sO_2 measurements:
2. Wavelengths should be selected within the Q-band of the hemoglobin absorption spectrum (i.e., 550-600 nm) to ensure a sufficient signal-to-noise ratio and adequate penetration.
3. Wavelengths where the absorption coefficients of HbO_2 and HbR have a pronounced difference (e.g., HbR-dominant 561 nm and HbO_2 -dominant 578 nm) are recommended.

Besides sO_2, HbT can be calculated by adding [HbR] and [HbO_2] together, or it can be directly measured at isosbestic wavelengths of the molar extinction coefficient spectra of hemoglobin (e.g., 530 nm, 545 nm, 570 nm, and 584 nm)[14], where HbR and HbO_2 have equal molar extinction coefficients.

5. Representative Results:

Shown in Figure 1 is the vascular anatomy and sO_2 in a living nude mouse ear imaged by dual-wavelength (561 and 570 nm) OR-PAM. The typical image acquisition time for dual-wavelength sO_2 measurements of such a region of interest (image size: 10 mm x 10 mm; step size: 2.5 μm x 5 μm) is ~80 min.

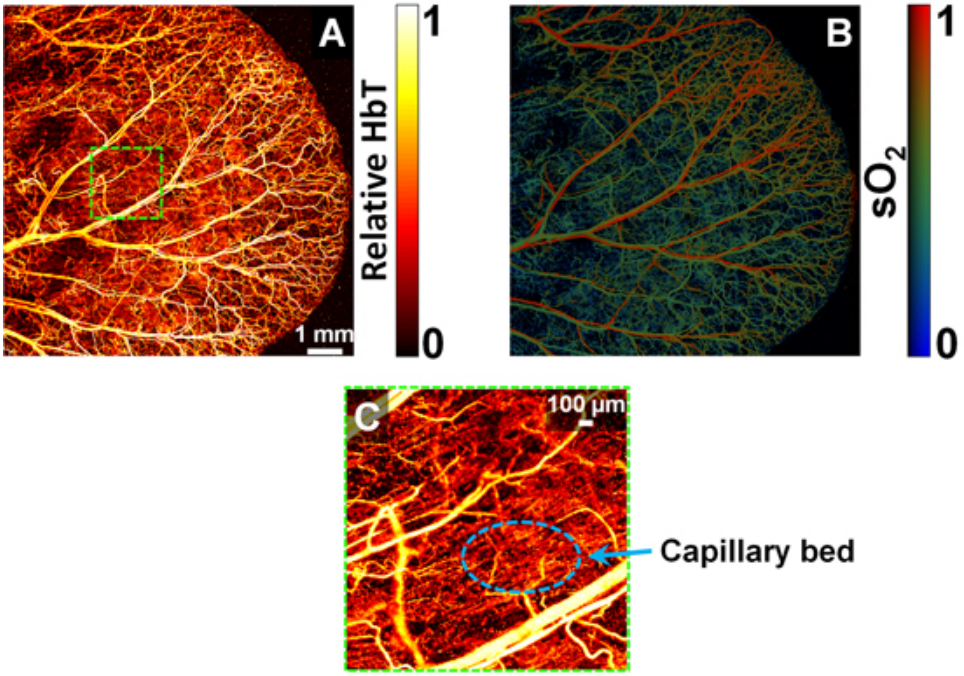

Figure 1. *In vivo* optical-resolution photoacoustic microscopy. MAP images of (A) the total hemoglobin concentration showing the vascular anatomy (acquired at 570 nm) and (B) the hemoglobin oxygen saturation (acquired at 561 nm and 570 nm) in a nude mouse ear. (C) Close-up of the boxed region in panel (A). The scale bar in panel (A) applies to both (A) and (B).

Discussion

In this video, we provide a detailed instruction on the experimental protocols of OR-PAM, including system configuration, system alignment, and typical experimental procedures. Label-free, noninvasive OR-PAM has enabled studies of microvascular functioning and metabolism on a single capillary basis and thereby holds the potential to expand our understanding of microcirculation-related physiology and pathology. Microphotoacoustics is currently manufacturing this OR-PAM system.

Disclosures

All experimental animal procedures were carried out in conformance with the laboratory animal protocol approved by the School of Medicine Animal Studies Committee of Washington University in St. Louis.

Acknowledgements

The authors appreciate Dr. Lynnea Brumbaugh's close reading of the manuscript. This work was sponsored by National Institutes of Health Grants R01 EB000712, R01 EB008085, R01 CA134539, U54 CA136398, and 5P60 DK02057933. Prof. Lihong V. Wang has a financial interest in Microphotoacoustics, Inc. and Endra, Inc., which, however, did not support this work.

References

1. Maslov, K., Zhang, H. F., Hu, S., and Wang, L. V. Optical-resolution photoacoustic microscopy for *in vivo* imaging of single capillaries. Opt. Lett. 33(9), 929-931 (2008).
2. Zhang, C., Maslov, K. and Wang, L. V. Subwavelength-resolution label-free photoacoustic microscopy of optical absorption *in vivo*, Opt. Lett. 35(19), 3195-3197 (2010).
3. Wang, Y., Maslov, K., Kim, C., Hu, S., and Wang, L. V. Integrated photoacoustic and fluorescence confocal microscopy. IEEE. Trans. Biomed. Eng. 57(10), 2576-2578 (2010).
4. Jiao, S., Xie, Z., Zhang, H. F., and Puliafito, C. A. Simultaneous multimodal imaging with integrated photoacoustic microscopy and optical coherence tomography. Opt. Lett. 34(19), 2961-2963 (2009).
5. Hu, S., Maslov, K., Tsytsarev, V., and Wang, L. V. Functional transcranial brain imaging by optical-resolution photoacoustic microscopy. J. Biomed. Opt. 14(4), 040503 (2009).
6. Hu, S., Yan, P., Maslov, K., Lee, J.M., and Wang, L. V. Intravital imaging of amyloid plaques in a transgenic mouse model using optical-resolution photoacoustic microscopy. Opt. Lett. 34(24), 3899-3901 (2009).
7. Hu, S., Rao, B., Maslov, K., and Wang, L. V. Label-free Photoacoustic Ophthalmic Angiography. Opt. Lett. 35(1), 1-3 (2010).
8. Jiao, S. L., Jiang, M. S., Hu, J. M., Fawzi, A., Zhou, Q. F., Shung, K. K., Puliafito, C. A., and Zhang, H. F. Photoacoustic ophthalmoscopy for *in vivo* retinal imaging. Opt. Express 18(4), 3967-3972 (2010).
9. Oladipupo, S., Hu, S., Santeford, A., Yao, J., Kovalski, J. R., Shohet, R., Maslov, K., Wang, L. V., and Arbeit, J. M. Conditional HIF-1 induction produces multistage neovascularization with stage-specific sensitivity to VEGFR inhibitors and myeloid cell independence. Blood (in press).
10. Hu, S., Maslov, K., and Wang, L. V. *In vivo* functional chronic imaging of a small animal model using optical-resolution photoacoustic microscopy. Med. Phys. 36(6), 2320-2323 (2009).
11. Hu, S., Maslov, K., and Wang, L. V. Second-generation optical-resolution photoacoustic microscopy with improved sensitivity and speed. Opt. Lett. 36(7), 1134-1136 (2011).

12. Wang, X., Pang, Y., Ku, G., Xie, X., Stoica, G., and Wang, L. V. Noninvasive laser-induced photoacoustic tomography for structural and functional *in vivo* imaging of the brain," Nat. Biotechnol. 21(7), 803-806 (2003).
13. Laser Institute of America, American National Standard for Safe Use of Lasers ANSI Z136.1-2007. American National Standards Institute Inc., New York, NY (2007).
14. Jacques, S. L., and Prahl, S. A. http://omlc.ogi.edu/spectra/hemoglobin/index.html.

